Supplementary Information for

Multifunctional *in vivo* vascular imaging using near-infrared II fluorescence

Guosong Hong[1,3], Jerry C. Lee[2,3], Joshua T. Robinson[1], Uwe Raaz[2], Liming Xie[1], Ngan F. Huang[2], John P. Cooke[2] & Hongjie Dai[1]

[1] Department of Chemistry, Stanford University, Stanford, California 94305, USA

[2] Division of Cardiovascular Medicine, School of Medicine, Stanford University, Stanford, California 94305, USA

[3] These authors contribute equally to this work.

Supplementary Figures

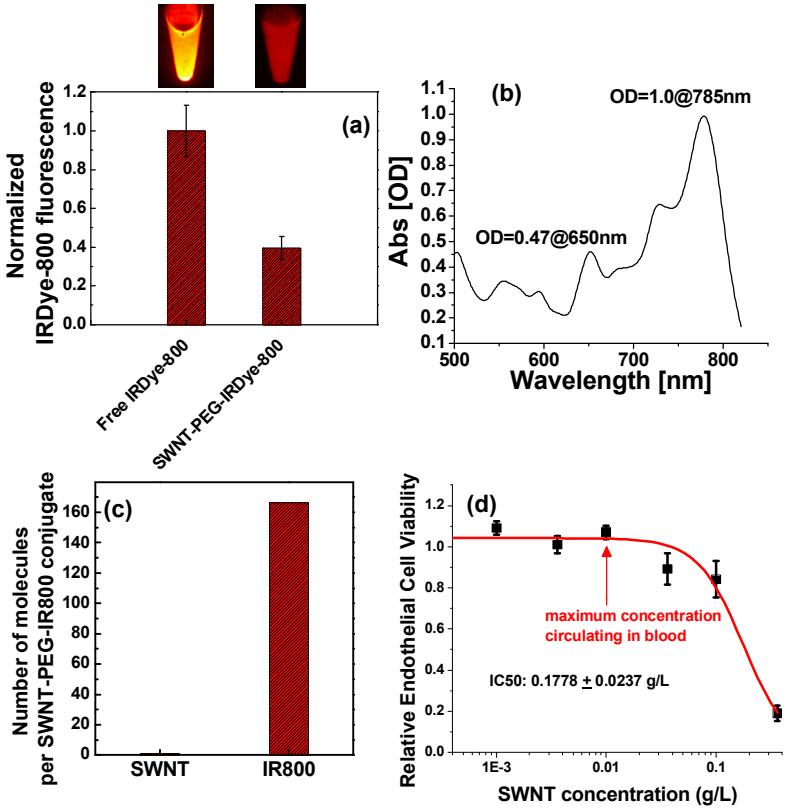

Figure S1. Chemical composition and cytotoxicity of SWNT-PEG-IRDye-800 conjugate. (**a**) Normalized IRDye-800 fluorescence for free IRDye-800 and SWNT-PEG-IRDye-800 at the same concentration of IRDye-800, suggesting the photoluminescence of IRDye-800 was quenched by ~60% due to the attachment to SWNTs through the PEG-chains. Inset pictures on top are corresponding photoluminescence images taken in the NIR-I window. (**b**) UV-Vis-NIR absorption spectrum of SWNT-PEG-IRDye-800 conjugate taken in a 1 mm cuvette, where the OD values at 650 nm and 785 nm are used for calculating the average number of SWNT and IRDye-800 molecules in SWNT-PEG-IRDye-800 conjugate. (**c**) Calculated number of SWNT and IRDye-800 molecules in each SWNT-PEG-IRDye-800 conjugate, indicating on average 167 IRDye-800 molecules on each SWNT backbone. The large number of IRDye-800 molecules attached to SWNTs ensured sufficient NIR-I emitters despite fluorescence quenching of IRDye-800 of ~60% in **a**. (**d**) Determination of half maximal inhibitory concentration (IC50) of SWNTs for endothelial cells. Original data (black squares) were fitted to sigmoidal function, revealing an IC50 value of 0.1778±0.0237 g/L. Errors bars reflect the standard deviation of relative endothelial cell viability values from 3 wells of cells incubated at the same SWNT concentration.

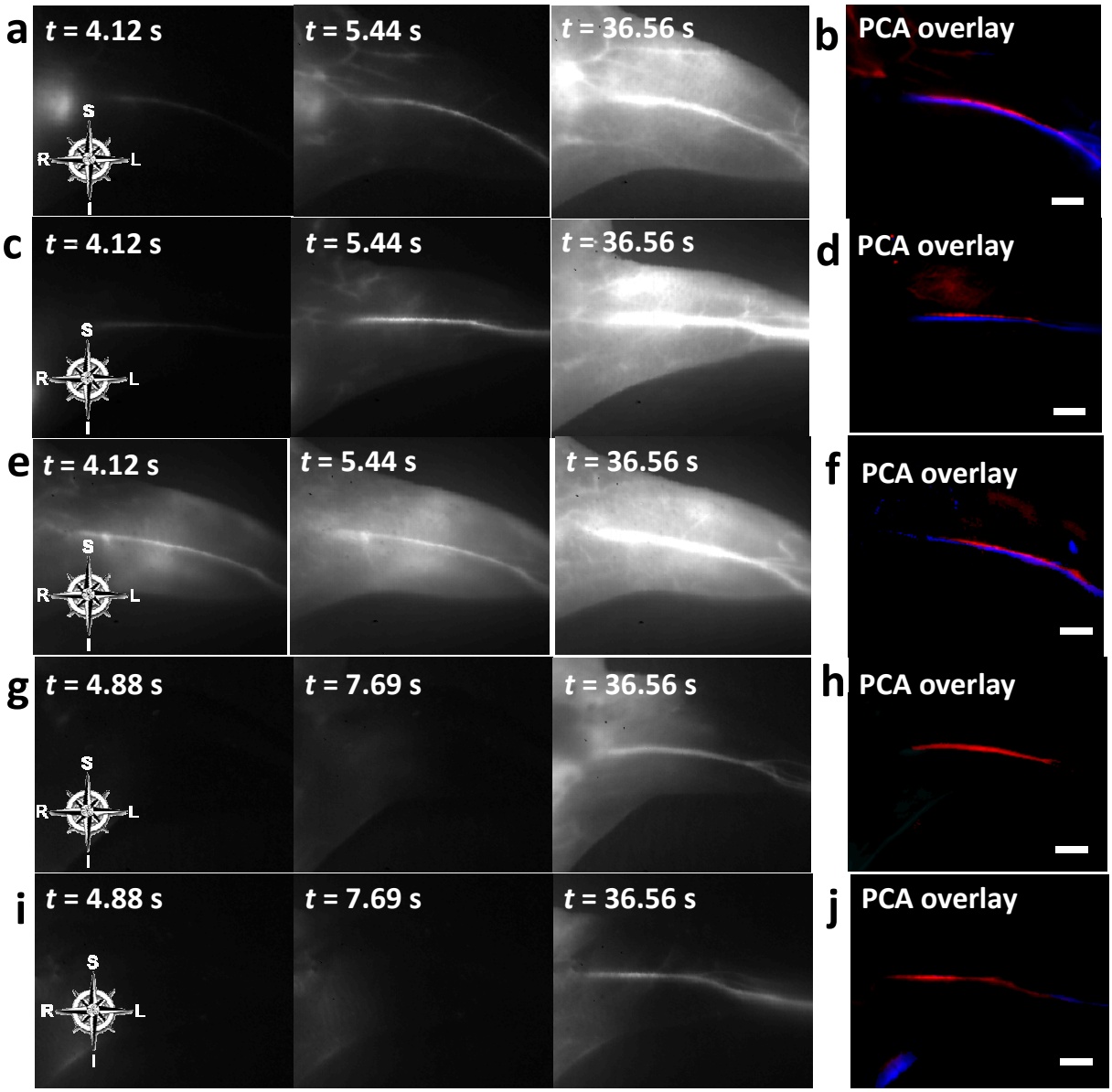

Figure S2. Differentiation of femoral artery and vein inside healthy, control hindlimbs of Mouse C2–4 (**a–f**) and ischemic hindlimbs of Mouse I2–3 (**g–j**). (**a,c,e,g,i**) Time course NIR-II fluorescence images showing hindlimb blood flow labeled by SWNT fluorescent tags. (**b,d,f,h,j**) PCA overlaid images based on the first 200 frames (37.5 s post injection) of each mouse, where arterial vessels are shown in red, while venous vessels are shown in blue. The scale bars all indicate 2 mm.

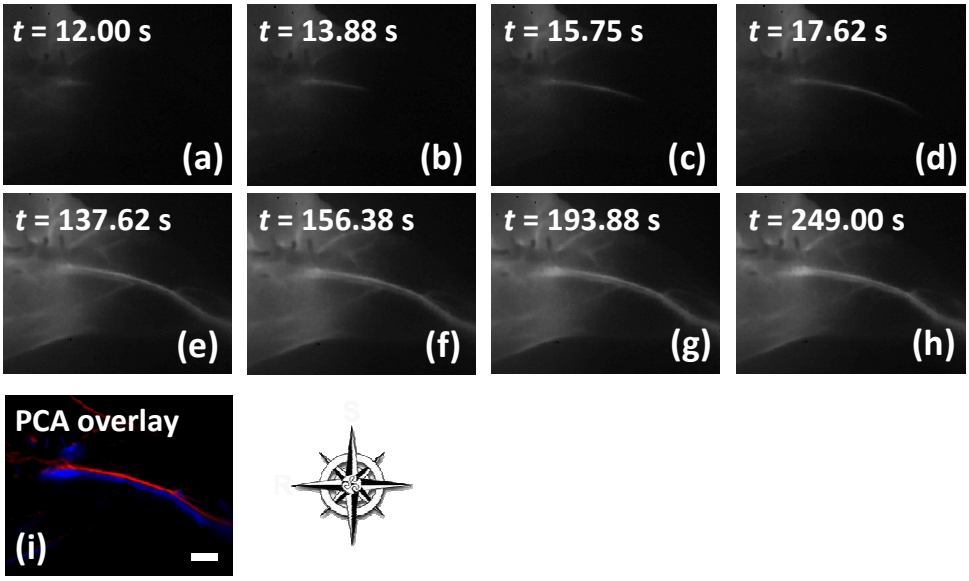

Figure S3. Differentiation of femoral artery and vein inside an ischemic hindlimb of Mouse I1 based on a longer post-injection imaging time. (**a**–**h**) Time course NIR-II fluorescence images showing hindlimb blood flow labeled by SWNT fluorescent tags. Note that femoral vein does not show up until after 2 min due to reduced blood flow of ischemia. (**i**) PCA overlaid image based on 1320 frames (up to 247.5 s post injection) of the mouse, where arterial vessels are shown in red, while venous vessels are shown in blue. The scale bar indicates 2 mm.

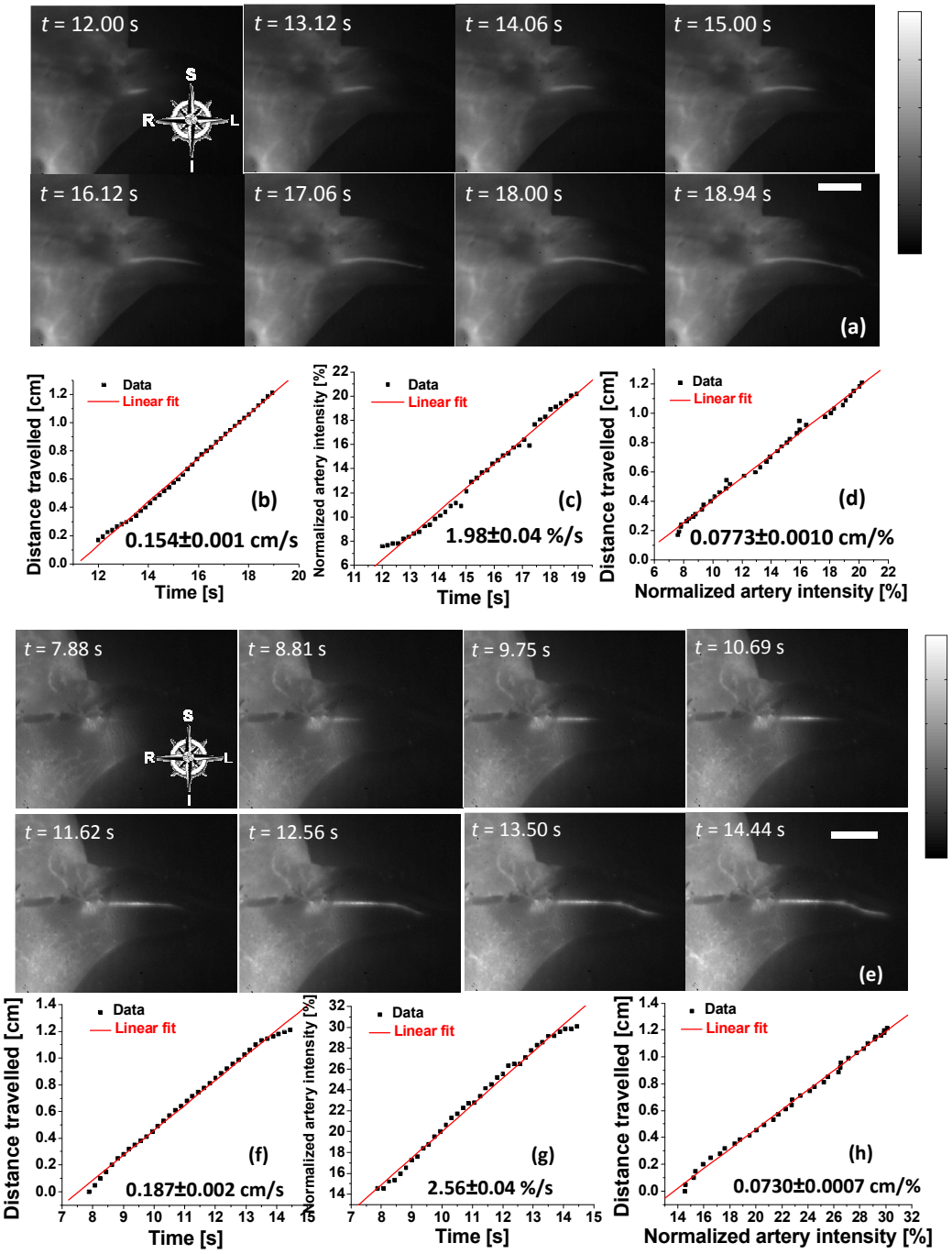

Figure S4. Arterial blood velocity analysis on the hindlimbs of ischemic Mouse I2 (**a-d**) and I3 (**e–h**). (**a,e**) NIR-II fluorescence images showing the flow front labeled by SWNT fluorescent tags. (**b,f**) Distance travelled by the flow front plotted as a function of time. (**c,g**) Normalized NIR-II signal in the femoral artery plotted as a function of time. (**d,h**) Linear correlation between the artery blood velocity and NIR-II fluorescence increase in the corresponding artery area. Scale bars in **a,e** indicate 5 mm and the intensity scale bars range from 0 to 1.

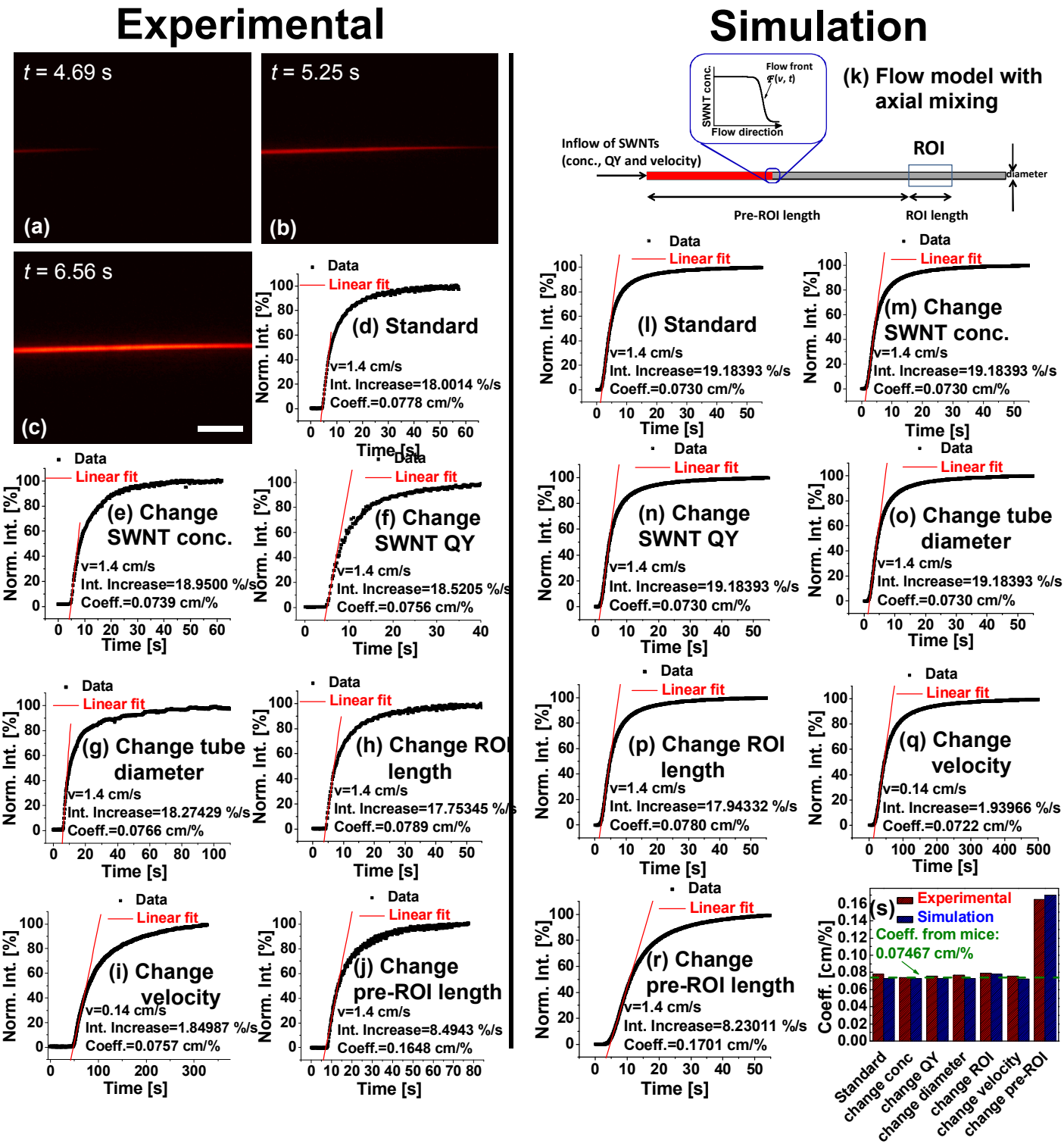

Figure S5. Variable dependency study of the intensity-to-velocity conversion coefficient based on both experimental (**a-j**) and simulation (**l-r**) results of the tubing flow setup (**k**). To find which variable(s) influence(s) the value of the coefficient, six possible parameters are changed one at a time from the

standard settings while keeping all other parameters unchanged. The standard settings are given by: SWNT concentration = 0.10 mg/mL, SWNT fluorescence quantum yield (QY) = 2.5%, tubing diameter = 760 μm, tubing length within ROI (i.e., ROI length) = 2.5 cm, fluid velocity = 1.4 cm/s and tubing length before ROI (i.e., pre-ROI length) = 8.5 cm. (**a-c**) NIR-II fluorescence images of SWNTs flowing through the tubing at 4.69 s, 5.25 s and 6.56 s post injection. Scale bar indicates 5 mm. (**d-j**) Experimental normalized NIR-II intensity increase curve as a function of time when: at the standard settings (**d**), only the SWNT concentration is reduced by 4 times (**e**), only the QY of SWNT is increased by 2 times (**f**), only the tubing diameter is reduced by 2 times (**g**), only the ROI length is reduced by 2 times (**h**), only the fluid velocity is reduced by 10 times (**i**), and only the pre-ROI is increased by 2 times (**j**). A linear fit based on the onset increase in each case gives a coefficient of 0.0778 cm/%, 0.0739 cm/%, 0.0756 cm/%, 0.0766 cm/%, 0.0789 cm/%, 0.0757 cm/% and 0.1648 cm/%, respectively. Note the coefficient remains invariant except in the case of a change in the pre-ROI length. (**k**) A schematic drawing of the tubing flow experiment setup, where all six parameters are labeled. The same setup is used in the numerical simulation, and the flow front is simulated by a sigmoidal function, the shape of which is dependent of both time and fluid velocity, based on a tubing flow model with axial mixing.[1,2] (**l-r**) Simulational normalized NIR-II intensity increase curve as a function of time when at the standard settings (**l**), only the SWNT concentration is reduced by 4 times (**m**), only the QY of SWNT is increased by 2 times (**n**), only the tubing diameter is reduced by 2 times (**o**), only the ROI length is reduced by 2 times (**p**), only the fluid velocity is reduced by 10 times (**q**), and only the pre-ROI is increased by 2 times (**r**). A linear fit based on the onset increase in each case gives a coefficient of 0.0730 cm/%, 0.0730 cm/%, 0.0730 cm/%, 0.0730 cm/%, 0.0780 cm/%, 0.0722 cm/% and 0.1701 cm/%, respectively. Note the coefficient remains invariant except in the case of a change in the pre-ROI length. (**s**) A bar chart summarizing the conversion coefficients derived from experimental results (red bars) and simulation (blue bars), with comparison to the coefficient derived from the femoral arterial flow in mice (green dashed line), showing the conversion coefficient invariant of SWNT concentration, SWNT quantum yield, tubing diameter, ROI length and fluid velocity, while only influenced by the pre-ROI length.

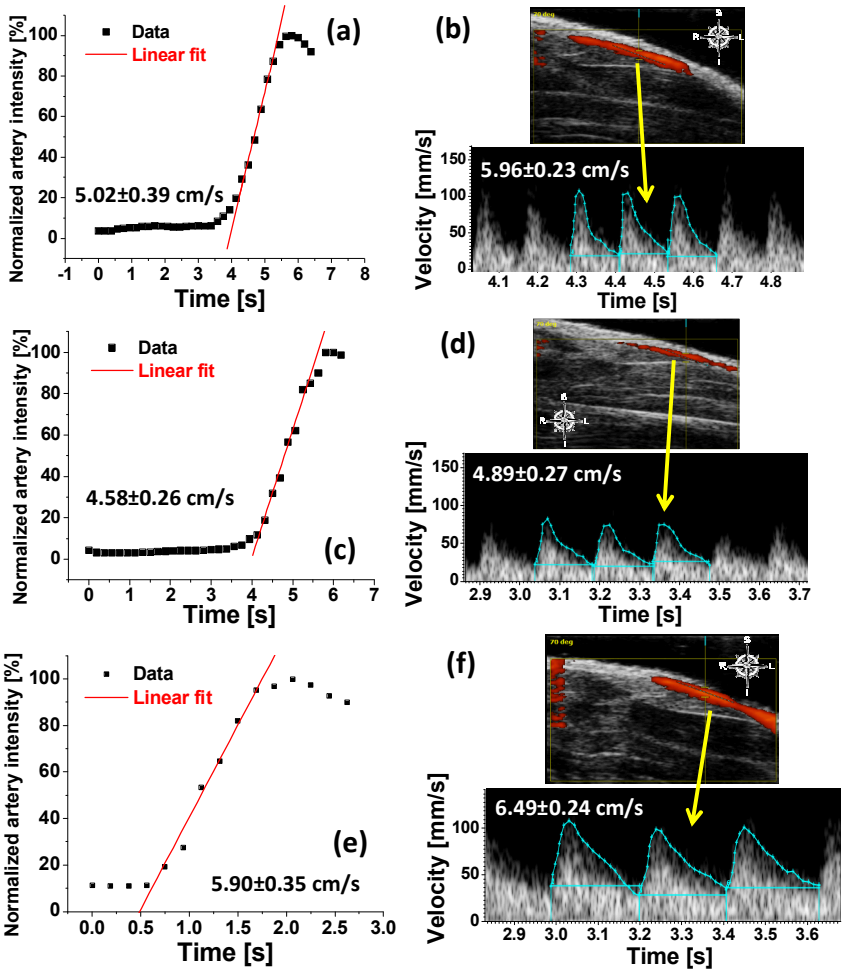

Figure S6. Reproduced femoral artery blood flow quantification in three healthy, control nude mice (Mouse C2–4). (**a**) Normalized NIR-II signal in the femoral artery plotted as a function of time, revealing a blood velocity of 5.02±0.39 cm/s after conversion for Mouse C2. (**b**) Power Doppler of femoral artery blood flow in Mouse C2 shown in the top graph, revealing an average blood velocity of 5.96±0.23 cm/s, based on the velocity time integral (VTI) of three cardiac cycles as shown by pulsed wave Doppler in the bottom graph. (**c**) Normalized NIR-II signal in the femoral artery plotted as a function of time, revealing a blood velocity of 4.58±0.26 cm/s after conversion for Mouse C3. (**d**) Power Doppler of femoral artery blood flow in Mouse C3 shown in the top graph, revealing an average blood velocity of 4.89±0.27 cm/s, based on the VTI of three cardiac cycles as shown by pulsed wave Doppler in the bottom graph. (**e**) Normalized NIR-II signal in the femoral artery plotted as a function of time, revealing a blood velocity of 5.90±0.35 cm/s after conversion for Mouse C4. (**f**) Power Doppler of femoral artery blood flow in Mouse C4 shown in the top graph, revealing an average blood velocity of 6.49±0.24 cm/s, based on the VTI of three cardiac cycles as shown by pulsed wave Doppler in the bottom graph.

References for SI

1 Zhao, L. L., Derksen, J. & Gupta, R. Simulations of Axial Mixing of Liquids in a Long Horizontal Pipe for Industrial Applications. *Energ. Fuel* **24**, 5844-5850 (2010).

2 Quinn, J. G. Modeling Taylor dispersion injections: Determination of kinetic/affinity interaction constants and diffusion coefficients in label-free biosensing. *Anal. Biochem.* **421**, 391-400 (2012).